Available online at www.sciencedirect.com
ScienceDirect
Progress in Natural Science 18 (2008) 441–446
Progress in Natural Science
www.elsevier.com/locate/pnsc

Analysis of contact melting around a horizontal elliptical cylinder heat source

Miao Gong, Wenzhen Chen *, Yuansong Zhao, Bo Zhu, Fengrui Sun

College of Power and Shipping, Naval University of Engineering, Wuhan, Hubei 430033, China

Received 20 August 2007; received in revised form 16 October 2007; accepted 22 October 2007

Abstract

The process of ΔT-driven contact melting of the solid phase change material (PCM) around a horizontal elliptical cylinder heat source is analyzed. Aiming at the problem existed in the published literature, namely the thickness of boundary layer tends to be infinite at $\phi = 90°$, and considering the difference of normal angle between the horizontal elliptical cylinder surface and the solid–liquid interface of PCM, a new mathematic model is proposed, and the fundamental equations for the melting process are derived with the film theory. The new pressure distribution inside the boundary layer, the variation law of normal angle of the solid–liquid interface, the thickness of the boundary layer and the relationship between the melting velocity and resultant force are obtained. The solutions of the fundamental equations under different elliptical compression coefficients are analyzed and discussed. It is found that the thickness of the boundary layer obtained by the new model is a finite value and accords with the experimental result at $\phi = 90°$.

Keywords: Contact melting; Elliptical cylinder; Phase change phenomena; Heat transfer

1. Introduction

The phenomena of contact melting of solid phase change material (PCM) around the heat source exist in nature and technological fields widely, such as weld, nuclear technology and heat control of spacecrafts etc. [1]. Many scholars have done a mass of researches on the processes of contact melting with different geometry shapes because of its high thermal conductivity and engineering application value. For example, Refs. [2–12] have given a series of useful analyses and experiments and numerical calculation results for the processes of contact melting that is driven by the temperature difference ΔT, around a heat source with different shapes, such as spherical, cylindrical, parabolic or elliptical shapes. Whereas all these studies adopt the homological analysis model, and result in that the thickness of the boundary layer tends to be infinite at $\phi = 90°$. It obviously does not accord with the practical phenomena and is needed to be improved. In the present work, the contact melting processes of PCM around a horizontal elliptical cylinder heat source are studied. Considering the difference of normal angle between the horizontal elliptical cylinder surface and the solid–liquid interface of PCM, we propose a new mathematic model and derive the fundamental equations for the melting process. The new variation law of the thickness and pressure distribution inside the boundary layer as well as the relationship between the melting velocity and resultant force are given.

2. Model and fundamental equations

The physical model and coordinates considered in this investigation are shown in Fig. 1. The radius of the elliptical cylinder heat source with compression coefficient

* Corresponding author. Tel.: +86 27 62537436.
E-mail address: cwz2@21cn.com (W. Chen).

1002-0071/$ - see front matter © 2007 National Natural Science Foundation of China and Chinese Academy of Sciences. Published by Elsevier Limited and Science in China Press. All rights reserved.
doi:10.1016/j.pnsc.2007.10.010

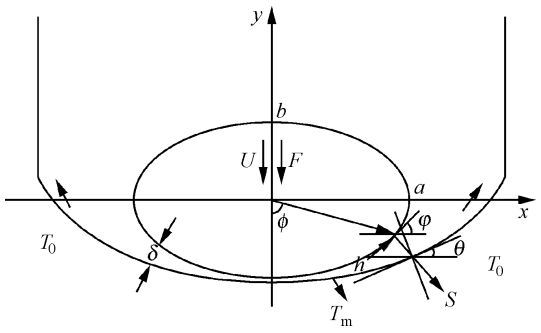

Fig. 1. Physical model and coordinates.

$J(J = b/a)$ on coordinate axis x and y is a and b, respectively. The horizontal elliptical heat source with the constant wall temperature T_w, on which a resultant force F is imposed, melts down through the PCM with the temperature T_0 at the constant velocity U. T_m is the melting point temperature of PCM. The angle between the radius of ellipse and negative axis y is noted by ϕ, which varies from 0° to 90°. The ellipse's tangent and normal are figured by h and S, respectively, and each is endued with the direction as shown in Fig. 1. φ is the angle between the ellipse's tangent and axis x, and θ is the angle between the tangent on the solid–liquid interface of PCM and axis x. It is assumed that (1) the thickness δ of melt liquid layer is so thin ($\delta \ll a,b$) that the pressure P in S direction inside the boundary layer can be supposed to be constant; (2) the inertia force is negligible as compared with viscous force, and heat transport by convective flow inside the boundary layer is also negligible as compared with that by heat conduction. Other assumptions are the same as Refs. [2–6].

The ellipse equation is

$$\frac{x^2}{a^2}+\frac{y^2}{b^2}=1 \tag{1}$$

The dominant equations of the melting processes inside the boundary layer are

$$\frac{\partial u}{\partial h}+\frac{\partial v}{\partial S}=0 \tag{2}$$

$$\mu\frac{\partial^2 u}{\partial S^2}=\frac{\mathrm{d}P}{\mathrm{d}h} \tag{3}$$

$$u\frac{\partial T}{\partial h}+v\frac{\partial T}{\partial S}=\alpha\frac{\partial^2 T}{\partial S^2} \tag{4}$$

The related boundary conditions are

$$\begin{aligned} &S=0: u=v=0 \quad T=T_w \\ &S=\delta: u=0, \quad v=-U\cos\theta, \quad T=T_m \end{aligned} \tag{5}$$

where u and v are the velocities of melt liquid along h and S directions inside the boundary layer, respectively. The energy balance equation in the solid–liquid interface is

$$-\lambda\frac{\partial T}{\partial S}|_{S=\delta}\cos(\varphi-\theta)=\rho L_m U\cos\theta \tag{6}$$

where $L_m = L + c_p(T_w - T_m)$ is the modified melting latent heat of PCM, and c_p is the specific heat of PCM.

Combining Eqs. (3) and (5), we can get

$$u=\frac{1}{2\mu}\frac{\mathrm{d}P}{\mathrm{d}h}(S^2-S\delta) \tag{7}$$

The mass balance equation inside the liquid boundary layer is

$$\int_0^\delta u\,\mathrm{d}s=\int_0^\phi U\cos\theta\,\mathrm{d}h \tag{8}$$

Substituting Eq. (7) into Eq. (8) yields

$$\frac{\mathrm{d}P}{\mathrm{d}h}=-\frac{12\mu U}{\delta^3}\int_0^\phi \cos\theta\,\mathrm{d}h \tag{9}$$

Because the thickness of the boundary layer is very thin, it is assumed that the temperature inside the liquid boundary layer is a linear distribution in S direction. Then from Eq. (5), we can get

$$T=T_w+\frac{T_m-T_w}{\delta}S \tag{10}$$

Substituting Eq. (6) into Eq. (10) yields

$$\delta=\frac{\alpha Ste\cos(\varphi-\theta)}{U\cos\theta} \tag{11}$$

where $Ste = c_p(T_w - T_m)/L_m$, and α is the thermal diffusivity of PCM.

If the temperature is approximated by a quadratic polynomial in S, the parameter Ste in Eq. (11) can be substituted by the following equation:

$$f(Ste)=\left(\sqrt{9Ste^2+280Ste+400}-3Ste-20\right)\Big/4 \tag{12}$$

When Ste is very small, $f(Ste)$ tends to be Ste, and there is no obvious difference between linear and quadratic polynomial distribution of the temperature.

The force F acting on the elliptical cylinder is

$$F=2\int_0^{\pi/2} P\cos\varphi\,\mathrm{d}h \tag{13}$$

From Fig. 1, we can derive the geometric relationship as follows:

$$\frac{\mathrm{d}\delta}{\mathrm{d}h}=\mathrm{tg}(\varphi-\theta) \tag{14}$$

From the ellipse curve, we can get the geometric relationship as follows:

$$\mathrm{tg}\varphi=J^2\mathrm{tg}\phi \tag{15}$$

$$\mathrm{d}h=\sqrt{\frac{1+J^4\mathrm{tg}^2\phi}{1+J^2\mathrm{tg}^2\phi}}\frac{aJ}{\cos^2\phi+J^2\sin^2\phi}\mathrm{d}\phi \tag{16}$$

The dimensionless parameters are defined as follows:

$$\begin{aligned} &\delta^*=\delta/a; \quad P^*=Pa^2/\mu\alpha \\ &U^*=Ua/\alpha; \quad F^*=Fa/\mu\alpha \end{aligned} \tag{17}$$

Substituting Eqs. (15) and (16) into Eqs. (8), (11), (13) and (14), respectively, we can derive

$$\frac{\mathrm{d}\delta^*}{\mathrm{d}\phi} = \sqrt{\frac{1+J^4\mathrm{tg}^2\phi}{1+J^2\mathrm{tg}^2\phi}}\frac{J^2\mathrm{tg}\phi - \mathrm{tg}\theta}{J^2\mathrm{tg}\phi\mathrm{tg}\theta + 1}\frac{J}{\cos^2\phi + J^2\sin^2\phi} \tag{18}$$

$$\delta^* = \frac{Ste}{U^*\sqrt{1+J^4\mathrm{tg}^2\phi}}(1 + J^2\mathrm{tg}\phi\mathrm{tg}\theta) \tag{19}$$

$$\frac{\mathrm{d}P^*}{\mathrm{d}\phi} = -\frac{12U^*}{\delta^{*3}}\sqrt{\frac{1+J^4\mathrm{tg}^2\phi}{1+J^2\mathrm{tg}^2\phi}}\frac{J}{\cos^2\phi + J^2\sin^2\phi} \times \int_0^{\phi}\cos\theta\sqrt{\frac{1+J^4\mathrm{tg}^2\phi}{1+J^2\mathrm{tg}^2\phi}}\frac{J}{\cos^2\phi + J^2\sin^2\phi}\mathrm{d}\phi \tag{20}$$

$$F^* = 2\int_0^{\frac{\pi}{2}} P^*\sqrt{\frac{1}{1+J^2\mathrm{tg}^2\phi}}\frac{J}{\cos^2\phi + J^2\sin^2\phi}\mathrm{d}\phi \tag{21}$$

Eqs. (18)–(21) are the new fundamental equations obtained for ΔT-driven contact melting around a horizontal elliptical cylinder. The unknown parameters in Eqs. (18)–(21) are P^*, δ^*, U^* and θ, which can be calculated with boundary conditions $\theta = 0°$, at $\phi = 0°$; $P^* = 0$, at $\phi = 90°$.

3. Solutions and analysis

There are no analytical solutions for Eqs. (18)–(21), and the numerical calculation is needed. The main steps are (a) giving an F^*, and temporarily endowing U^* with a proper value; (b) substituting Eq. (19) into Eq. (18) to eliminate δ^* and deriving equation $\mathrm{d}\theta/\mathrm{d}\phi = f(\theta, \phi)$; (c) using the initial conditions to obtain the limit of $\mathrm{d}\theta/\mathrm{d}\phi$ at $\phi \to 0°$; (d) calculating θ by the implicit difference method with the precision 1E-8, and obtaining δ^* from Eq. (19); (e) calculating P^* by the trapezoid stereometry and explicit difference method; (f) calculating a new F^* by the trapezoid stereometry from Eq. (21); (g) comparing the new calculated F^* with the given F^*, until the error is smaller than 10E-8 the calculation is finished. Then, we will get the solutions of Eqs. (18)–(21) with initial conditions.

Figs. 2–4 give the graphs of parameters obtained by the numerical calculation of Eqs. (18)–(21), which indicate the variation law of P^*, θ and δ^* along with ϕ under a different compression coefficient J while the elliptical cylinder is imposed on a constant resultant force, respectively. From Fig. 2, it can be seen that under the condition of a constant outside force, when $J > 5$, P^* descends sharply from the value at $\phi = 0°$ to a value nearby zero and then nearly keeps constant on the rest segment of the curve at larger ϕ. From Fig. 3, it can also be found that under the same condition as above, the variation law of θ along with ϕ has a flat opposite process to P^*s. Furthermore, when $J > 5$, the variation curves of the two parameters with ϕ change very little in values and shapes. The calculation shows that when $J < 0.2$ and $J > 20$, the variation curve of δ^* with ϕ is analogous to that of P^* with ϕ. Fig. 5 also shows the influence of J on the curve of U^*–F^*.

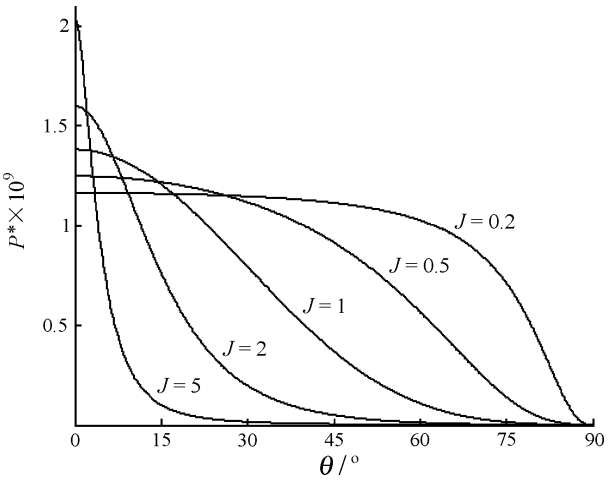

Fig. 2. The effect of J on variation curve of P^* with ϕ, when $F^* = 15 \times 10^{-8}$ and $Ste = 0.5$.

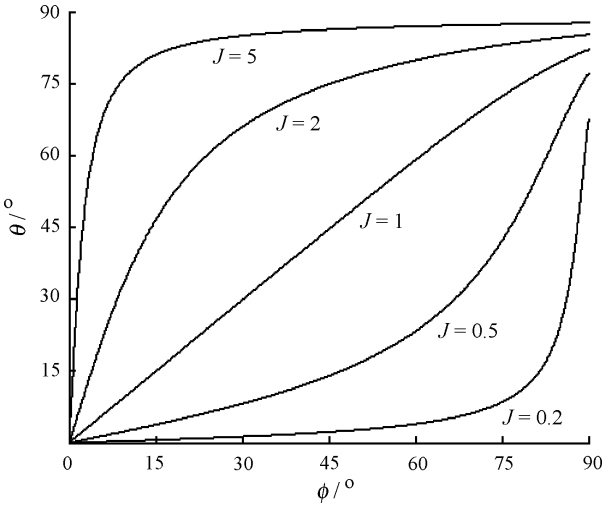

Fig. 3. The effect of J on variation curve of θ with ϕ, when $F^* = 15 \times 10^{-8}$ and $Ste = 0.5$.

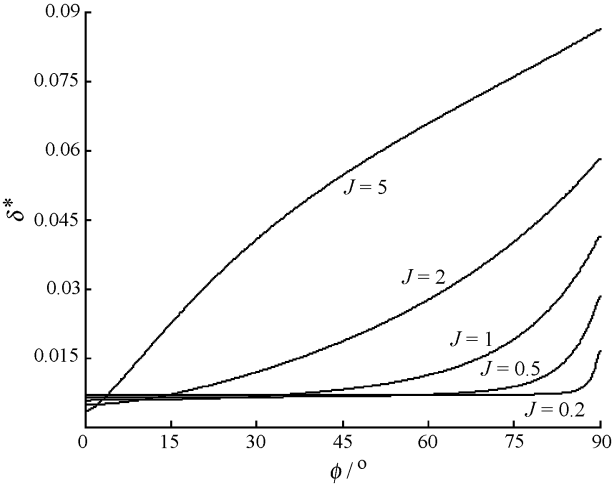

Fig. 4. The effect of J on variation curve of δ^* with ϕ, when $F^* = 15 \times 10^{-8}$ and $Ste = 0.5$.

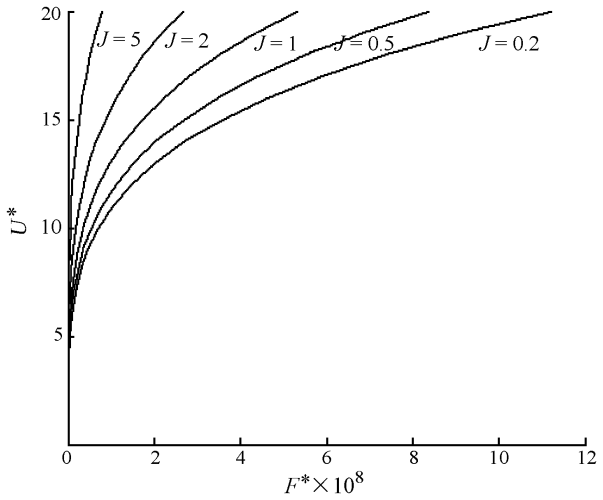

Fig. 5. The effect of J on variation curve of U^* with F^*, when $Ste = 0.1$.

Suppose $J = 1$, from Eqs. (18)–(21) we can get

$$\frac{d\delta^*}{d\phi} = \mathrm{tg}(\phi - \theta) \tag{22}$$

$$\delta^* = \frac{Ste\cos(\phi - \theta)}{U^*\cos\theta} \tag{23}$$

$$\frac{dP^*}{d\phi} = -\frac{12U^*}{\delta^{*3}}\int_0^{\phi}\cos\theta\, d\phi \tag{24}$$

$$F^* = 2\int_0^{\frac{\pi}{2}} P^*\cos\phi\, d\phi \tag{25}$$

Eqs. (22)–(25) are the new fundamental equations of contact melting process around a cylindrical heat source. The comparison of the results calculated by Eqs. (22)–(25) with Ref. [3]'s is shown in Figs. 6 and 7.

For the contact melting around a plate in PCM, we have [13]

$$F^* = 8U^{*4}/Ste^3 \tag{26}$$

$$\delta^* = Ste/U^* \tag{27}$$

Figs. 8 and 9 give the related curves of δ^*–ϕ and U^*–F^*, which are, respectively, calculated from Eqs. (18)–(21) with $J = 0.01$ and Eqs. (26) and (27). From Fig. 8, it is clear that

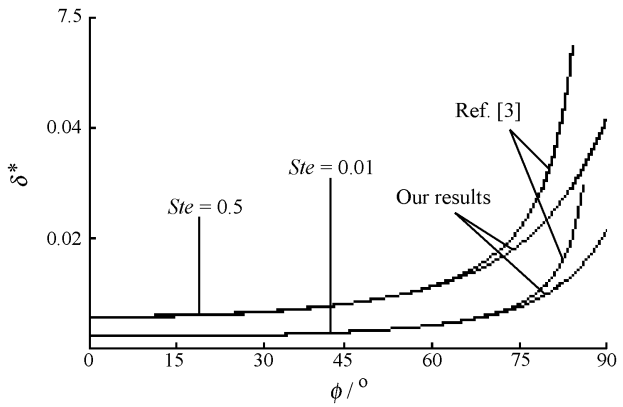

Fig. 6. The distribution of thickness of boundary layer with different Ste, when $F^* = 15 \times 10^{-8}$ and $J = 1$.

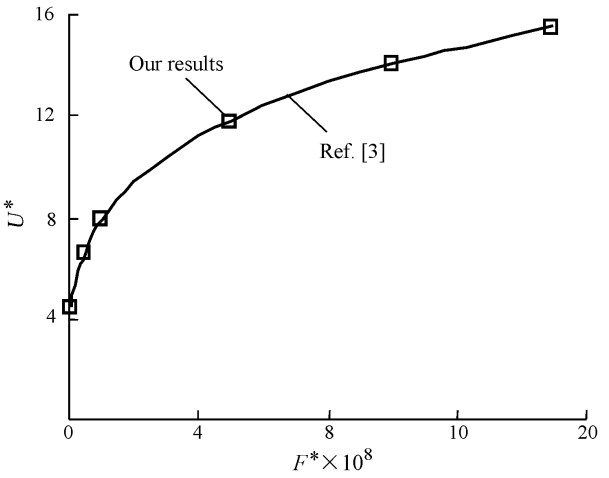

Fig. 7. The variation curve of U^* with F^*, when $Ste = 0.05$.

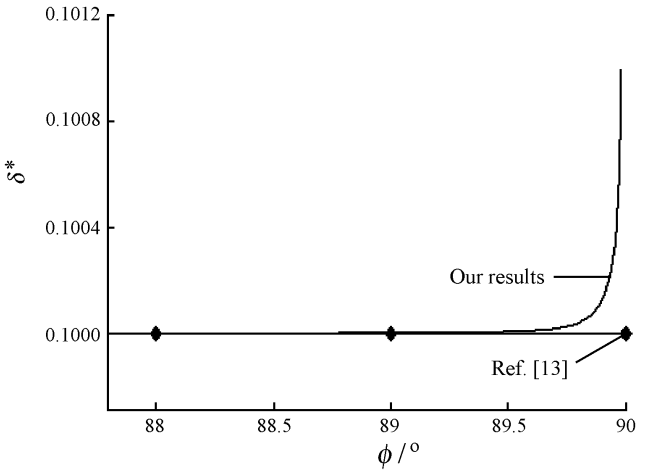

Fig. 8. The distribution of thickness of boundary layer, when $U^* = 1$, $J = 0.01$ and $Ste = 0.1$.

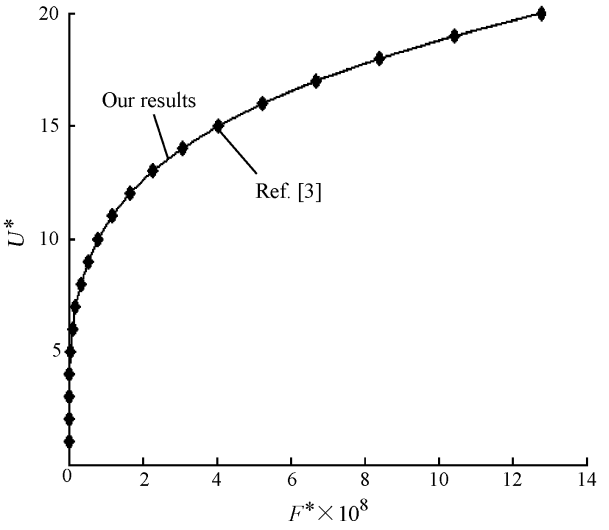

Fig. 9. The variation of U^* with F^*, when $Ste = 0.1$ and $J = 0.01$.

the two curves keep superposition until ϕ draws near 90°, and at $\phi = 90°$ the value of δ^* by Eqs. (18)–(21) is larger about 1% than that by Eqs. (26) and (27). When $J = 0.01$, from Fig. 9 it can also be seen that two curves nearly keep superposition. But when the curves were magnified, the value of U^* by Eqs. (18)–(21) is appreciably bigger than that by Ref. [13]'s under the same F^* condition. Calculating and comparing the curves of δ^*–ϕ and U^*–F^* with different J illustrates that the curves of δ^*–ϕ and U^*–F^* for $J < 0.1$ are the same as shown in Figs. 8 and 9. So when $J < 0.1$, the elliptical cylinder can be considered as a flat plate for the contact melting around PCM.

Suppose $\theta = \varphi$, from Eqs. (9) and (11) we can get

$$\frac{dP}{dh} = -\frac{12\mu U}{\delta^3}x \tag{28}$$

$$\delta = \frac{\alpha Ste}{U\cos\varphi} \tag{29}$$

Eqs. (28) and (29) are the fundamental equations derived by Ref. [11] under the same supposition condition.

Fig. 10 is the graph of δ^*–ϕ obtained by Eqs. (18)–(21) and Ref. [11] under the conditions of the same U^* and Ste. Fig. 10 or calculating shows that (a) when $J < 1$, the two curves keep superposition while ϕ is below a certain angle ϕ_o which increases with the decrease of J, but our curve is upon the Ref. [11]'s while $\phi > \phi_o$; (b) when $J > 1$, our curve is always upon Ref. [11]'s. It is need to point out that the dimensionless thickness δ^* obtained by Eqs. (18)–(21) reaches a certain value at $\phi = 90°$, but δ^* obtained by Ref. [11] will tend to the infinite at $\phi = 90°$ as shown in Fig. 10.

Fig. 11 is the graph of U^*–F^* obtained by Eqs. (18)–(21) and Ref. [11] under the condition of the same Ste. No matter what the value of J is, our curve is always under Ref. [11]'s, which will be clearer with the increase of J.

Fig. 12 shows the photo taken from our experiment of ΔT-driven contact melting. Obviously, the thickness of the boundary layer is finite on the two sides of the elliptical cylinder. And the experimental value approximates to our theoretical results. While $\phi = 90°$, under the experimental conditions the value of δ^* calculated by Eqs. (18)–(21) is 0.077, and the experimental results are shown in Table 1.

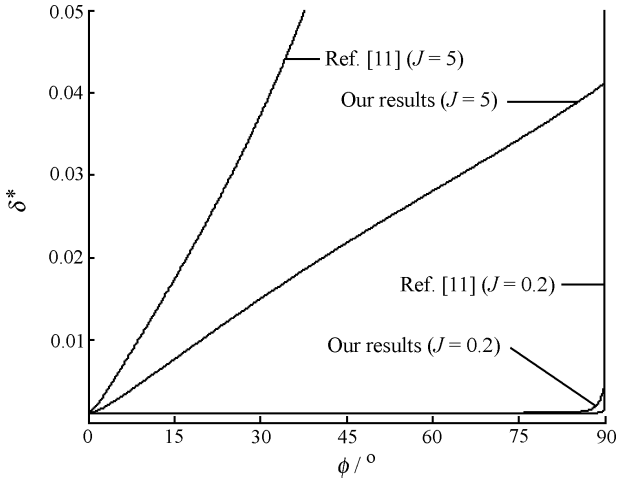

Fig. 10. The variation curve of δ^* with ϕ, when $U^* = 89.51$ and $Ste = 0.1$.

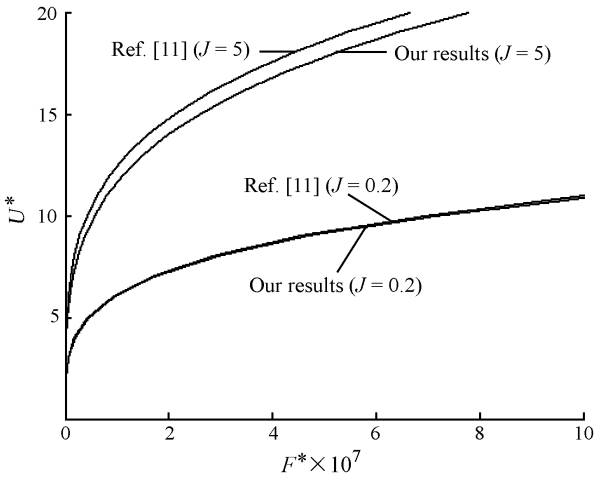

Fig. 11. The variation curve of U^* with F^*, when $Ste = 0.1$.

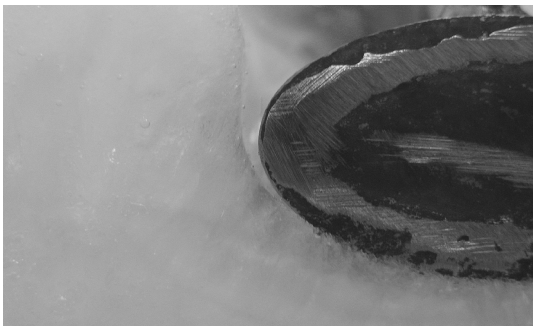

Fig. 12. ΔT-driven contact melting of *n*-octadecane around an elliptical cylinder, when $J = 0.5$.

Table 1
The experimental results at $\phi = 90°$

	1	2	3	4	5	6
δ^*	0.0635	0.0862	0.0801	0.0737	0.0769	0.0900

Though there are still differences between the theoretical and experimental results, the amelioration by our above new model is obvious, namely, the value of δ^* is finite at $\phi = 90°$.

4. Conclusions

P^*, δ^*, F^*, U^* and θ are all the important parameters during the process of contact melting of PCM around a horizontal elliptical heat source. In this paper, the mathematical model is improved, and the new fundamental equations are derived with the film theory. The new pressure distribution inside the boundary layer, the variation law of normal angle of the solid–liquid interface, the thickness of the boundary layer and the relationship between the melting velocity and

resultant force are obtained for different values of J. The results indicate that after considering the difference of normal angle between the horizontal elliptical cylinder surface and the solid–liquid interface, the thickness of the boundary layer on the two sides of the elliptical cylinder can be worked out with a certain value. So we suggest that Eqs. (18)–(21) be employed in the researches of variation law of the thickness of the boundary layer, by which there will be a more reasonable and accurate result than that by the published literatures. But when $J < 0.1$, because the equations derived by Ref. [13] are more convenient for us to use, the elliptical cylinder can be taken as a flat plate if the thickness of the boundary layer near $\phi = 90°$ is not calculated. Also when $J < 0.5$, it is suggested to use the mathematical model of Ref. [11] because of its tiny difference and convenience. For the other J, the mathematical model and equations can be chosen according to the requirement.

Acknowledgement

This work was supported by National Natural Science Foundation of China (Grant No. 50376074).

References

[1] Bejan A. Contact melting heat transfer and lubrication. Adv Heat Transfer 1994;24:1–38.
[2] Emerman SH, Turcotte DL. Stokes's problem with melting. Int J Heat Mass Transfer 1983;26(11):1625–30.
[3] Moallemi MK, Viskanta R. Melting around a migrating heat source. J Heat Transfer 1985;107:451–9.
[4] Moallemi MK, Viskanta R. Experiments on flow induced by melting around a migrating heat source. J Fluid Mech 1985;157:35–51.
[5] Moallemi MK, Viskanta R. Analysis of close contact melting heat transfer. Int J Heat Mass Transfer 1986;29(6):855–67.
[6] Moallemi MK, Viskanta R. Analysis of melting around a moving heat source. Int J Heat Mass Transfer 1986;29(8):1271–82.
[7] Vargas JVC, Bejan A, Dobrovicescu A. The melting of an ice shell on a heated horizontal cylinder. J Heat Transfer 1994;116:702–8.
[8] Pudovcin MA, Salamatin AN, Fomin SA, et al. Effect of a thermal drill on hot-point ice boring performance. J Soviet Math 1988;43(3):2496–505.
[9] Fomin SA, Cheng SM. Optimization of the heating surface shape in the contact melting problem. In: Dulikravich GS, editor. Proceedings of third international conference on inverse design concepts and optimization in engineering sciences, Washington DC, October 23–25, 1991. p. 136–143.
[10] Chen WZ, Cheng SM, Gu WM. Heat transfer problem during the self-burial process of a parabolic nuclear waste container. Nucl Tech 1995;18(1):40–4, [in Chinese].
[11] Chen WZ, Cheng SM, Luo Z. An analytical solution of melting around a moving elliptical heat source. J Ther Sci 1994;3(1):23–7.
[12] Hu YJ, Shi MH. Analysis of melt-film thickness profile in PCM solid close-contact melting around a hot sphere. Acta Energ Solaris Sin 1998;19(1):74–9, [in Chinese].
[13] Chen WZ, Yang QS. The analysis of contact melting of ice under a flat plate. Acta Energ Solaris Sin 1999;20(2):162–6, [in Chinese].